THE JOURNAL OF PHYSICAL CHEMISTRY C

Article

pubs.acs.org/JPCC

Calorimetric Study of Alkali Metal Ion (K^+, Na^+, Li^+) Exchange in a Clay-Like MXene

Geetu Sharma,[†] Elayaraja Muthuswamy,[†] Michael Naguib,[‡] Yury Gogotsi,[∥] Alexandra Navrotsky,*[,†] and Di Wu[†,§]

[†]Peter A. Rock Thermochemistry Laboratory and NEAT ORU, University of California Davis, Davis, California 95616, United States

[‡]Materials Science and Technology Division, Oak Ridge National Laboratory, Oak Ridge, Tennessee 37381, United States

[§]The Gene and Linda Voiland School of Chemical Engineering and Bioengineering, Washington State University, Pullman, Washington 99163, United States

[∥]A. J. Drexel Nanomaterials Institute and Department of Materials Science and Engineering, Drexel University, Philadelphia, Pennsylvania 19104, United States

Supporting Information

ABSTRACT: Intercalation of ions in layered materials has been explored to improve the rate capability in Li-ion batteries and supercapacitors. This work investigates the energetics of alkali ion exchange in a clay-like MXene, $Ti_3C_2T_x$, where T_x stands for anionic surface moieties, by immersion calorimetry in aqueous solutions. The measured immersion enthalpies of clay-like $Ti_3C_2T_x$, ΔH_{imm}, at 25 °C in 1 M KCl, 1 M NaCl, 1 M LiCl, and nanopure water are −9.19 (±0.56), −5.90 (±0.31), −1.31 (±0.20), and −1.29 (±0.13) kJ/mol of MXene, respectively. Inductively coupled plasma mass spectrometry is used to obtain the concentrations of alkali ions in the solid and aqueous phases. Using these concentrations, the enthalpies of exchange of alkali metal ions (Li^+, Na^+, and K^+) are calculated; ΔH_{ex} in 1 M KCl, 1 M NaCl, 1 M LiCl, and nanopure water are −9.3 (±2.2), 21.0 (±0.9), −1.3 (±0.2), and 302.4 (±0.6) kJ/mol of MXene, respectively. Both immersion and exchange enthalpies are most exothermic for potassium. This suggests that K^+ ions interact more strongly with anions present in the interlayers of this MXene than Na^+ and Li^+ ions. Water vapor adsorption calorimetry indicates very weak interaction of water with the MXene, while immersion calorimetry suggests a weakly hydrophilic nature of the MXene surface.

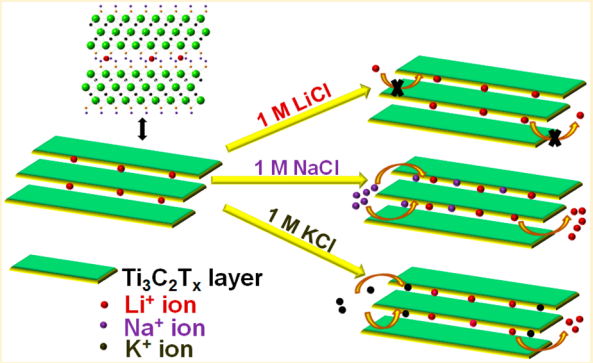

INTRODUCTION

Freestanding two-dimensional (2D) structures have garnered significant attention for applications in energy storage and electronics. The widely studied materials of this type have mostly been derived by exfoliation of layered materials such as graphite,[1] hexagonal BN,[2] and MoS_2.[3] More complex structures composed of more than one element are currently explored targeting new properties, and MXenes have been a major addition to the family of 2D materials.[4] MXenes are usually derived from layered ternary or quaternary carbides such as MAX phases, by selective extraction chemistry where the main group element (A-layer) is etched out by an acid treatment, typically using HF-containing solutions.[5,6] The MAX phases can be described by a general molecular formula $M_{n+1}AX_n$ (n = 1−3) and are composed of alternately stacked hexagonal close-packed $M_{n+1}X_n$ blocks interleaved with atomic A layers. Since the first report on a Ti_3C_2 MXene, a number of other MXene compounds have been reported.[7] The etching leads to surface termination with functional groups such as OH, O, and F, resulting in weakly bound $M_{n+1}X_n$ layers. Subsequent delamination of these layers, after intercalation, by sonication or just shaking in water results in the formation of single- or few-layer MXene flakes.[8,9] Though it is tempting to call the MXene produced from Ti_3AlC_2 (assuming complete removal of Al and no other elements present) Ti_3C_2, the real composition is much more complicated and variable, although this variation is not often characterized.[10−12]

Extensive efforts have been dedicated to developing materials with higher capacities and longer lifetimes than the currently used graphite anodes in Li-ion batteries and carbon based electrodes for electrochemical capacitors. Layered materials are attractive for these applications due to the combination of their flat surfaces and the large interlayer surface areas.[13,14] Among 2D materials, MXenes offer a rare combination of metallic conductivity in the sheets, ion exchange and hydration between the layers, and redox capability. Functionalized MXenes have

Received: March 14, 2017
Revised: June 6, 2017
Published: June 21, 2017

DOI: 10.1021/acs.jpcc.7b02419
J. Phys. Chem. C 2017, 121, 15145−15153

been reported to be very good electrical conductors.[15] There have been many reports claiming that they are indeed promising anode materials for Li-ion batteries.[8,16−18] Delaminated MXene based Li-ion anodes exhibited much higher reversible capacities of 400−600 $mAhg^{-1}$.[8,19,20] A volumetric capacity of 1375 $mAhcm^{-3}$ (635 $mAhg^{-1}$) was obtained for PVP-Sn(IV)@Ti_3C_2 electrodes.[21] A high capacity of about 1250 $mAhg^{-1}$ at 0.1 C was achieved by a porous $Ti_3C_2T_x$/CNT composite electrode.[22] So far, the best electrochemical performance has been shown by $Ti_3C_2T_x/NiCo_2O_4$ films having a reversible capacity of 1330 $mAhg^{-1}$ at 0.1 C.[23] However, predictions from DFT on Li-ion intercalation of functionalized Ti−C MXenes have provided smaller values of Li-ion storage capacity than the experimental observations.[24−28]

Ghidiu et al.[17] were able to successfully etch the Al from Ti_3AlC_2 using a solution of LiF in 6 M HCl. Notably, unlike MXene synthesized using HF, the LiF-HCl etching resulted in MXene that exhibits clay-like properties. When dry, it is a free-flowing powder, but when wet, it behaves like a clay that can be rolled and deformed into thin sheets. X-ray diffraction (XRD) measurements confirmed a larger *c*-lattice parameter when compared to the HF etched MXene (28 vs 20 Å). In addition, the hydrated MXene had even larger *c*-lattice parameters up to 40 Å, suggesting intercalation of water and cations between the $M_{n+1}X_n$ layers.[29]

Recent reports have addressed the effect of intercalation mechanisms of various metal ions in MXenes. Osti et al.[30] suggested, on the basis of complementary X-ray and neutron scattering techniques along with molecular dynamics simulations, that intercalation of K^+ ions yields a MXene with more uniform and homogeneous structure. This is claimed to be due to the water molecules in the K^+ intercalated MXene becoming much less mobile, thereby increasing stability.[30] Kajiyama et al.[31] have demonstrated reversible Na^+ intercalation/deintercalation into the interlayer space of $Ti_3C_2T_x$ in a nonaqueous Na^+ electrolyte. Mashtalir et al.[32] have shown that hydrazine intercalation into a $Ti_3C_2T_x$ leads to a change in the surface functional groups and intercalated water molecules. Ahmed et al.[33] reported that treatment of a $Ti_3C_2T_x$ with H_2O_2 results in swelling or opening of layers, significantly improving performance in Li-ion batteries. In addition, the theoretical sodium storage capacity of bare and functionalized Ti−C MXenes significantly increases on expanding their interlayer distances.[34] Ren et al.[35] demonstrated nonpermeability to cations with hydration radii larger than the interlayer spacing and high selectivity toward single, double, and triple charged metal and dye cations in $Ti_3C_2T_x$ membranes. Thus, it is clear that the nature of intercalated species greatly alters MXene properties. However, the energetics which governs the extent of intercalation or ion exchange and the stability of MXenes on intercalation is still unknown. Obtaining quantitative thermochemical data on intercalation and exchange reactions in $Ti_3C_2T_x$ is the goal of the present study.

Immersion calorimetry and water adsorption calorimetry are very useful methods to probe the energetics associated with intercalation, adsorption, and confinement of H_2O and other small molecules and ions in porous and layered materials.[36−39] The heat of immersion/adsorption depends on the surface area and porosity of the material and the specific interactions of the molecules/ions with the surface, pore, and/or interlayer space. Both methods have been well established and utilized to study a wide range of porous and layered materials.[40−43] We apply them here to shed light on the adsorptive/intercalation energetics of a chemically well-characterized $Ti_3C_2T_x$.

In order to interpret heat effects per mole of sample or per mole of exchanging species, the complete elemental composition of MXene must be established. Elemental analysis was carried out on the sample used in immersion calorimetry, both before and after the immersion experiment, as well as on the aqueous solution after immersion. This allows writing chemically balanced reactions associated with the measured heat effects.

We have determined, using immersion calorimetry in an aqueous solution at room temperature, the enthalpies associated with uptake of different cations (Li^+, Na^+, K^+) by the clay-like $Ti_3C_2T_x$. The enthalpies of ion exchange were also studied by accounting for the intercalation and release of ions identified through pH measurements and ICP-MS analysis of the solid and solution samples. A single well characterized sample of overall composition $Ti_3Al_{0.21}C_2O_{0.81}(OH)_{0.06}F_{0.77}Cl_{0.02}Li_{0.38}$, as determined by chemical analysis, was used as the starting material. However, this sample contained some unreacted Ti_3AlC_2 in addition to AlF_3 remaining from the etching process of the MAX phase, as discussed in our prior paper on the heat of formation of $Ti_3C_2T_x$.[44] Therefore, immersion and exchange enthalpies were also calculated for the MXene composition $Ti_3C_2(OH)_{0.06}F_{0.25}O_{0.84}Cl_{0.02}Li_{0.38}$, after correction for the assumed impurities. In addition, water vapor adsorption calorimetry experiments on two different MXene samples were also performed and are discussed.

EXPERIMENTAL METHODS

Materials. Two different samples were synthesized at the Oak Ridge National Laboratory as described in our previous report.[44] The clay-like $Ti_3C_2T_x$ was prepared using LiF-6 M HCl solution as the etching agent.[17] The other method utilized dilute HF solution as an etchant.[6] In contrast to MXenes produced using HF by difficult handling of concentrated HF and the laborious steps of intercalation, delamination, and filtration, the clay-like MXene produced using LiF-HCl is simple to make. Both samples were analyzed for their surface area and water adsorption characteristics. The clay-like sample, after complete chemical analysis, was used for immersion calorimetry.

Surface Area Determination. The Brunauer−Emmett−Teller (BET) surface area was measured using a Micromeritics ASAP 2020 instrument (Micromeritics Corp, Norcross, GA). The samples were degassed at 200 °C for 18 h before the analysis. Five-point adsorption isotherms of nitrogen at −196 °C were collected in the $P/P°$ relative pressure range from 0.05 to 0.7, where $P°$ is the saturation pressure at −196 °C.

Water Adsorption Calorimetry. A Micromeritics2020 ASAP analyzer (Micromeritics Corp, Norcross, GA) in conjunction with a Setaram DSC111 Calvet microcalorimeter (Setaram Inc., Cailure, France) was used for the water adsorption enthalpy measurements. The technique enables simultaneous determination of the amount of water adsorbed and the enthalpy associated with the adsorption process.[45] The sample (~20 mg pellet) was introduced into one side of a thoroughly dried forked silica glass tube. The tube was inserted into the calorimeter such that each side is in one of the twinned calorimetric chambers. Before dosing water, the samples were degassed under vacuum at temperatures in the range 110−200 °C for 6−12 h. Each dose provided 2.0 μmol of water, and the equilibration time period was 90 min.

DOI: 10.1021/acs.jpcc.7b02419
J. Phys. Chem. C 2017, 121, 15145−15153

Immersion Calorimetry. The enthalpies of immersion of the MXenes in various aqueous solutions (water, 1 M KCl, 1 M NaCl, 1 M LiCl) were determined at 25.0 ± 0.5 °C using a Setaram C-80 twin microcalorimeter (Setaram Inc., Cailure, France). Hand-pressed pellets of the clay-like MXene (10−20 mg) were dropped into the aqueous solutions. The heat of interaction was recorded as a function of time. The return of the calorimetric signal to its initial value (baseline) indicated the completion of reaction. Typically measurement times varied from 30 to 70 min depending on the sample and solution. Multiple drops were made on each side of the calorimeter to establish the reproducibility of the measurement. At the end of the experiment, the sample (both solid and solution) was stored for further evaluation of changes in pH and ion concentrations.

pH Measurements and ICP-MS Analysis. pH measurements were carried out on the solutions before and after the immersion experiments. The pH electrode was calibrated on the day of measurements with neutral and acidic (pH 4.0) buffer solutions. The average of three consistent readings was used for quantifying moles of protons released per mole of the sample, and there was almost no variation between the three values.

ICP-MS measurements were carried out by the UC Davis Interdisciplinary Center for Plasma Mass Spectrometry using an Agilent 7500CE ICP-MS (Agilent Technologies, Palo Alto, CA). The samples were introduced using a MicroMist Nebulizer (Glass Expansion, Pocasset, MA) into a temperature-controlled spray chamber with helium as the collision cell gas. Instrument standards were diluted from Certiprep ME 2A (SPEX CertiPrep, Metuchen, NJ 08840) to 0.5, 1, 10, 100, 200, 500, 1000, 2000, and 5000 mg/L, respectively, in 3% trace element HNO_3 (Fisher Scientific) in 18.2 MΩ-cm water. A NIST 1643E standard (National Institute of Standards and Technology, Gaithersburg, MD) was analyzed initially, and quality control standards consisting of ME 2A at a concentration of 100 mg/L were analyzed every 12th sample as quality controls.

For ICP-MS sample preparation, solution samples were diluted so that the analyte of interest (Li, Na, K) is in the 100−1000 ppb range. Three dilutions were made for each sample, and the average value obtained was used in the calculations. In the case of solid samples, a known quantity of dried sample was completely digested in 20% HNO_3 solution. The MXene sample completely oxidized, yielding a white powder (oxidation to TiO_2) after overnight stirring at RT. The system was then centrifuged to isolate the solid, and the diluted solutions of the supernatant were used to measure the intercalated Li, Na, and K content.

Additional elemental analysis of the as-etched sample before the measurement was carried out by ICP-OES at Element Materials Technology, New Berlin, WI, USA. The carbon and sulfur contents were determined using a combustion/IR technique. The analysis for fluorine and chlorine content was carried out by SF Analytical Europhins Lab l, New Berlin, WI, USA, by method MIL-STD-2041.

Together, these analytical methods provided complete chemical analysis of both the solids and the solutions.

RESULTS AND DISCUSSION

XRD patterns for HF and HCl-LiF derived MXenes are shown in Figure S1 in the Supporting Information. In agreement with previous reports, the *c*-lattice parameters for HF and HCl-LiF derived MXenes were found to be ∼19.9 and 29.8 Å, respectively. BET measurements indicated a very low surface area for both samples: 6.45 ± 0.11 and 5.89 ± 0.09 m^2/g for the HF and HCl-LiF derived MXenes, respectively. Thus, the choice of etchant does not substantially affect their surface area. The interlayer spacing of MXenes is not accessible to nitrogen. On the basis of the first-principles calculations, the theoretical specific surface area (SSA) for a perfect Ti_2C with O termination is 671 m^2/g.[46] The experimental SSA of exfoliated Ti_2CT_x etched using HF is 23 m^2/g.[16] The SSA of exfoliated Ti_2CT_x with mesopores etched using LiF-HCl is 19.1 m^2/g.[46] That of another exfoliated sample is 20.2 m^2/g.[47] The SSA for $Ti_3C_2T_x$ etched using HF is reported as 13 m^2/g, which is higher than our measurements.[48] This may be because of the presence of TiO_2 nanoparticles on the Ti_3C_2 surface. The scatter in various reported data may reflect different preparation methods, particle sizes, and the possible presence of TiO_2 nanoparticles in some of the samples. The relatively low SSA of our samples suggests some agglomeration of particles. One would predict greater water adsorption on samples with larger SSA.

The water vapor adsorption isotherms, in the range of P/P° from 0.05 to 0.7 (Figure 1a), are of type III, indicating minimal water intake at low pressures. The first dose of water resulted in a differential enthalpy of −28.7 kJ/mol of H_2O for MXene prepared by HCl-LiF treatment (Figure 1b). Assuming the degas process at 110 °C eliminated all surface adsorbents and intercalated water molecules, the observed enthalpy would indicate a very weak interaction of water molecules with the MXene surface. The subsequent dosing of water indicates even less favorable interactions. The small enthalpies measured in these experiments clearly indicate the absence of chemisorption and could possibly be attributed to hydrophobic surface characteristics, perhaps due to the presence of fluoride. However, such hydrophobicity is not supported by contact angle measurements for MXenes produced by either HF or HCl-LiF and all previous work on $Ti_3C_2T_x$, which easily disperses in water and forms very stable solutions.[15,17,49] It is worth noting that in this study the measurements were carried out using water vapor (P/P° from 0.05 to 0.7) while all the

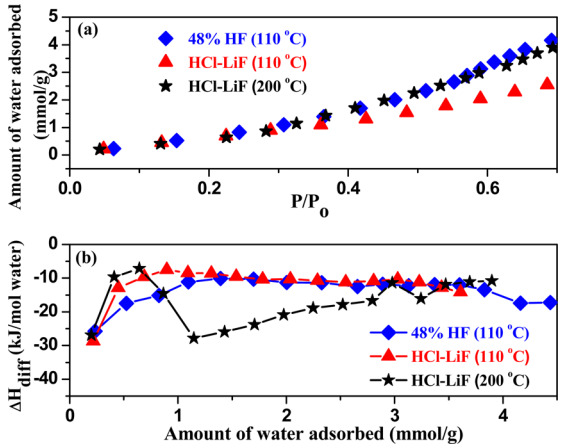

Figure 1. (a) Water vapor adsorption isotherms and (b) differential heat of adsorption as a function of the amount of water adsorbed. The degas temperatures are given in parentheses. The red and black traces correspond to MXene obtained by HCl-LiF treatment, and the blue trace corresponds to that obtained by HF treatment.

DOI: 10.1021/acs.jpcc.7b02419
J. Phys. Chem. C 2017, 121, 15145−15153

other studies used water in the liquid form for the contact angle measurements.

The weak interactions could also suggest that water vapor has not penetrated the interlayer space of the samples and all one observes is weak adsorption on external surfaces. This could be an intrinsic property of the samples, or it could be caused by incomplete removal of water during preparation and degassing. If it is because of an incomplete removal of water, it will be in agreement with what was reported by Ghidiu et al.[29] for an air-dried Li intercalated $Ti_3C_2T_x$. They found that there is no increase in the *c*-lattice parameter while increasing the relative humidity from 0 to 90%. Only at a relative humidity of more than 90%, a jump in the *c*-lattice parameter was observed.

To try to completely remove any intercalated water, the sample was subjected to a more extreme degas condition (12 h at 200 °C under vacuum). Once again, adsorption measurements were associated with low enthalpies (Figure 1b). The sample prepared by HF treatment also exhibited essentially identical adsorption characteristics (Figure 1a). Since these isotherms suggest unfavorable water adsorption, the slight changes in the isotherm for the HCl-LiF etched sample degassed at 200 °C may not provide unique information on differences in sample surfaces. Instead, they may simply indicate slight and possibly random variations in water clustering events. It is also possible that the surface is slightly different and the sample might undergo some changes upon heating at 200 °C. In any case, all samples show very weak water interactions. The results from our adsorption experiments appear to be inconsistent with the XRD measurements, which have shown that the clay-like $Ti_3C_2T_x$ has strong water adsorption, even with staging of water layers at a relative humidity of more than 90%.[29] However, if the strongly bound water is not removed during the degas process, the observations might be reconciled. Alternately, the lattice parameter variations may be caused by pillars of a small number of water molecules, rather than continuous layers of water surrounding the intercalated ions, or by the presence of salt/ions after etching.

Although there appear to be no direct studies of H_2O vapor adsorption in MXenes, there are various theoretical and experimental studies concerning adsorption of other gases. Xiao et al.[50] reported adsorption of NH_3 on MXenes using first-principles simulations. The results implied that NH_3 could be strongly adsorbed on M_2CO_2 MXene (M = Sc, Ti, Zr, and Hf) with apparent charge transfer which renders them potential candidates for NH_3 sensing or capture.[50] Yu et al.[51] investigated adsorption of NH_3, H_2, CH_4, CO, CO_2, N_2, NO_2, and O_2 on monolayer Ti_2CO_2 using first-principles simulations. Among all of these molecules, only NH_3 could be chemisorbed on the Ti_2CO_2 monolayer. Gao et al.[52] used density functional calculations to show that O terminations on the top and bottom layers of 2D MXenes act as catalytic active sites for hydrogen evolution reactions. Liu et al.[46] experimentally detected substantial CH_4 adsorption capacity for exfoliated Ti_2C with mesopores. Liu et al.[53] demonstrated superior catalytic effects of Ti_3C_2 toward the hydrogen storage reaction of MgH_2 compared to samples doped with other Ti-based materials. Density functional theory investigations suggested that M_3C_2 transition metal carbides of the d^2, d^3, and d^4 elements have promising N_2 capture behavior which displays spontaneous chemisorption, promoting its catalytic conversion into NH_3.[54] These studies appear to show relatively strong interactions of nitrogen-bearing species, especially ammonia, with titanium carbide based MXenes. The above adsorption studies suggest that MXenes are promising candidates for adsorption of various gas molecules and thus for energy storage and catalytic applications.

To avoid possible problems with difficult access of low-pressure water vapor to the interlayer space, we decided to measure MXene–water interactions by water immersion calorimetry using a large excess of aqueous solution, which better replicates synthesis conditions and applications where aqueous solutions are used such as supercapacitors. Furthermore, we could study the effect of different ionic species in solution, which are not accessible in vapor adsorption experiments. To interpret this series of immersion experiments, the analyzed elemental composition of the clay-like sample (Table S1 in the Supporting Information) was utilized.

On the basis of the elemental and ICP-MS analyses, the overall composition for the HCl-LiF MXene sample is $Ti_3Al_{0.21}C_2O_{0.81}(OH)_{0.06}F_{0.77}Cl_{0.02}Li_{0.38}$. Apportioning this composition to the phase impurities and more stoichiometric MXene (see our prior paper),[44] we get 3.08 wt % Ti_3AlC_2, 7.26 wt % AlF_3, and 89.66 wt % $Ti_3C_2(OH)_{0.06}F_{0.25}O_{0.84}Cl_{0.02}Li_{0.38}$. Assuming the phase impurities are inert and do not participate in the immersion reactions, 0.897 g of this MXene (molecular weight 190.178) is available to participate in the immersion and ion exchange per gram of sample. This assumption forms the basis of thermochemical calculations for the corrected composition.

Figure 2 is a schematic illustration of ion intercalation/deintercalation in the clay-like MXene. The calorimetric data

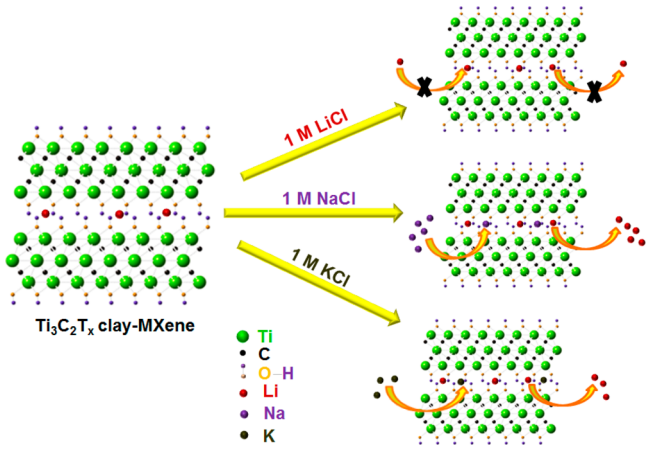

Figure 2. Schematic illustration of ion intercalation in a clay-like MXene.

support rapid ion exchange, as the immersion calorimetric peaks looked normal and did not show any long "tails" suggestive of slow reaction. The enthalpies of immersion in deionized water and 1 M alkali halide solutions at 25 °C for measured and impurity-corrected compositions are listed in Table 1. They show similar values and trends. The heat effects are consistently exothermic and small in magnitude. The average enthalpy of immersion in nanopure water for measured and corrected MXene composition is −1.29 ± 0.13 and −1.33 ± 0.13 kJ/mol, respectively. The reference state for water is liquid (not vapor). Since there is no straightforward way to obtain the amount of water entering the MXene, the enthalpy per mole of H_2O could not be calculated. The immersion calorimetry data imply small interaction of the MXene with water, indicating the surface is weakly hydrophilic and is

DOI: 10.1021/acs.jpcc.7b02419
J. Phys. Chem. C 2017, 121, 15145−15153

Table 1. Immersion Enthalpies (per Gram or Mole of MXene) of Clay-MXene with Deionized Water and 1 M Alkali Chloride Solutions at 25 °C

	ΔH_{imm},[a] J/g		ΔH_{imm},[b] kJ/mol	
solution	measured composition[c]	corrected composition[d]	measured composition	corrected composition
1 M KCl	−44.77 ± 2.85 (8)[e]	−49.94 ± 3.18	−9.19 ± 0.56	−9.50 ± 0.60
1 M NaCl	−28.76 ± 1.49 (8)	−32.08 ± 1.66	−5.90 ± 0.31	−6.10 ± 0.32
1 M LiCl	−6.38 ± 0.96 (11)	−7.07 ± 1.11	−1.31 ± 0.20	−1.34 ± 0.21
nanopure H_2O	−6.28 ± 0.61 (11)	−7.0 ± 0.68	−1.29 ± 0.13	−1.33 ± 0.13

[a] ΔH_{imm} = Enthalpy of immersion. [b] The formula weight established from the elemental composition is 205.244 g/mol for measured composition and 190.178 g/mol for corrected composition. [c] Measured composition: $Ti_3Al_{0.21}C_2O_{0.81}(OH)_{0.06}F_{0.77}Cl_{0.02}Li_{0.38}$. [d] Corrected composition for impurity phases: $Ti_3C_2(OH)_{0.06}F_{0.25}O_{0.84}Cl_{0.02}Li_{0.38}$. [e] The number of measurements is given in parentheses.

consistent with the contact angle measurements because the water is in liquid form in both cases.

The measurements in 1 M LiCl solution yield enthalpies similar to the values obtained with nanopure water. The average enthalpy for measured and corrected MXene composition is −1.31 ± 0.20 and −1.34 ± 0.21 kJ/mol, respectively. This is the same within error as the value in pure water. Since the MXene contains mainly lithium as the interlayer cation, there should be little heat associated with cation exchange of lithium between the solid and the solution. Apparently, there is also little heat associated with any possible ion exchange (H/F). Thus, the data in pure water and LiCl appear consistent with weak H_2O−MXene interactions.

The observed heat effects for the same sample in 1 M NaCl are −5.90 ± 0.31 and −6.1 ± 0.32 kJ/mol for measured and corrected compositions, respectively. In contrast, the heat effects in 1 M KCl are −9.19 ± 0.56 and −9.50 ± 0.60 kJ/mol for measured and corrected MXene, compositions, respectively. The heat effects in NaCl and KCl solutions are more exothermic than the values in water and LiCl. The correction for impurities has a negligible effect on the energetics for all of the experiments.

Figure 3 suggests a roughly linear dependence of the immersion enthalpy on the ionic radius of the desolvated alkali metal ion,[55] with potassium being the most exothermic. However, lithium, having the smallest ionic size, has the highest hydration enthalpy. Therefore, the immersion enthalpy appears to decrease in magnitude with the hydration enthalpy, perhaps suggesting that possible increasing hydration upon immersion is not the main energetic driver. Indeed, the observed enthalpies may be a sum of heat effects associated with various ion exchanges that take place during a measurement. These include intercalation of the alkali metal ion (K^+ or Na^+) and the release of Li^+, F^-, OH^-, and H^+ into the aqueous system. The observed heat effects can be fully understood only after a complete analysis of all of these possible exchanges.

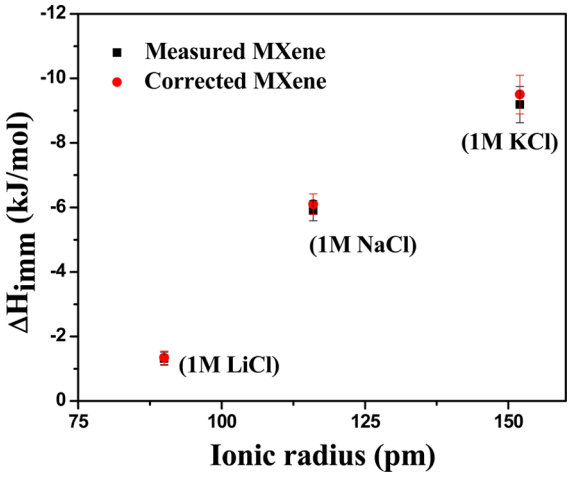

Figure 3. Immersion enthalpy of measured and corrected MXene compositions in various 1 M alkali chloride solutions. Ionic radius from ref 55.

As a first step to characterize the complex exchange reactions, pH measurements of all solutions were carried out before and after each series of immersion experiments (Tables S2 and S3 in the Supporting Information). All of the solutions were more acidic after interaction with the sample. In each case, two values are presented, corresponding to experiments in each reaction chamber of the twinned Calvet calorimeter; the values are consistent. Since no effort was made to exclude atmospheric CO_2, some acidity related to its aqueous solubility is expected, but the important observation is the difference in pH before and after the immersion experiment. The measured changes are used to quantify the amount of H^+ released per mole of sample (see Tables S2 and S3 in the Supporting Information). The extent of proton release was smallest in nanopure water. In the alkali solutions, proton release is higher by 1 order of magnitude and greatest in 1 M NaCl, but it is still small compared to the extent of ion exchange.

After completion of immersion calorimetry, all of the solutions and solid samples were collected and compositions were determined by ICP-MS analysis to quantify the extent of ion exchange (see Tables S4 and S5 in the Supporting Information). In all of the calculations, the average of the two values in each reaction chamber of the twinned calorimeter is taken. One control experiment on the solid sample was also carried out to check the lithium content (0.3978 mol of Li/mol of MXene). On the basis of this analysis, the expected sum of the Li^+ content from the solution and the solid should be 0.3978 (the initial Li content in the solid). However, there is a slight difference in all of the systems between the expected and observed values, but this is probably within experimental error of the initial composition and the ICP-MS analysis. The results clearly indicate that the clay-like MXene, initially containing Li^+ as its major cation, on contact with water and 1 M NaCl and 1 M KCl solutions releases Li^+ ions from MXene layers into the solutions. In addition, K^+ and Na^+ ions enter the MXene on contact with their corresponding alkali solutions. The measured Li content at the beginning (before any exchange) is possibly the maximum amount of ions, which can intercalate spontaneously in the clay-like MXene. In other words, the total amount of Li^+ and K^+ or Li^+ and Na^+ in the MXene after exchange should be equal to the number of Li^+ ions in the initial sample, namely, 0.38 for charge balance. Any extra K^+, Na^+, or Li^+ in the solid sample after the exchange reactions may

DOI: 10.1021/acs.jpcc.7b02419
J. Phys. Chem. C 2017, 121, 15145−15153

be in the form of salts precipitated on the MXene surface. In support of this hypothesis, precipitated KCl is seen by X-ray diffraction for a sample immersed in KCl, separated, and dried. The measured enthalpy shows there is almost zero driving force for any intercalation in 1 M LiCl.

On the basis of the ICP-MS measurements, the possible ion exchange reactions taking place between the clay-like MXene (measured composition; $Ti_3Al_{0.21}C_2O_{0.81}(OH)_{0.06}F_{0.77}Cl_{0.02}Li_{0.38}$) and the corresponding medium (nanopure water or alkali chloride solutions) are shown in eqs 1−4, which use the analyzed compositions.

In 1 M KCl:

$$Ti_3Al_{0.21}C_2O_{0.81}(OH)_{0.06}F_{0.77}Cl_{0.02}Li_{0.38} + 0.258\ K^+ \rightarrow Ti_3Al_{0.21}C_2O_{0.81}(OH)_{0.06}F_{0.77}Cl_{0.02}Li_{0.122}K_{0.258} + 0.258\ Li^+ \quad (1)$$

In 1 M NaCl:

$$Ti_3Al_{0.21}C_2O_{0.81}(OH)_{0.06}F_{0.77}Cl_{0.02}Li_{0.38} + 0.344\ Na^+ \rightarrow Ti_3Al_{0.21}C_2O_{0.81}(OH)_{0.06}F_{0.77}Cl_{0.02}Li_{0.036}Na_{0.344} + 0.344\ Li^+ \quad (2)$$

In 1 M LiCl:

$$Ti_3Al_{0.21}C_2O_{0.81}(OH)_{0.06}F_{0.77}Cl_{0.02}Li_{0.38} \rightarrow Ti_3Al_{0.21}C_2O_{0.81}(OH)_{0.06}F_{0.77}Cl_{0.02}Li_{0.38} \quad (3)$$

In nanopure H_2O:

$$Ti_3Al_{0.21}C_2O_{0.81}(OH)_{0.06}F_{0.77}Cl_{0.02}Li_{0.38} \rightarrow Ti_3Al_{0.21}C_2O_{0.81}(OH)_{0.06}F_{0.628}Cl_{0.02}Li_{0.238} + 0.142\ Li^+ + 0.142\ F^- \quad (4)$$

Similarly, the possible ion exchange reactions taking place between the composition-corrected MXene $Ti_3C_{2.0}(OH)_{0.06}F_{0.25}O_{0.84}Cl_{0.02}Li_{0.38}$ and the corresponding medium are described in eqs 5−8.

In 1 M KCl:

$$Ti_3C_2O_{0.84}(OH)_{0.06}F_{0.25}Cl_{0.02}Li_{0.38} + 0.2545\ K^+ \rightarrow Ti_3C_2(OH)_{0.06}F_{0.25}O_{0.84}Cl_{0.02}Li_{0.1255}K_{0.2545} + 0.2545\ Li^+ \quad (5)$$

In 1 M NaCl:

$$Ti_3C_2(OH)_{0.06}F_{0.25}O_{0.84}Cl_{0.02}Li_{0.38} + 0.343\ Na^+ \rightarrow Ti_3C_2(OH)_{0.06}F_{0.25}O_{0.84}Cl_{0.02}Li_{0.037}Na_{0.343} + 0.343\ Li^+ \quad (6)$$

In 1 M LiCl:

$$Ti_3C_2(OH)_{0.06}F_{0.25}O_{0.84}Cl_{0.02}Li_{0.38} \rightarrow Ti_3C_2(OH)_{0.06}F_{0.25}O_{0.84}Cl_{0.02}Li_{0.38} \quad (7)$$

In nanopure H_2O:

$$Ti_3C_2(OH)_{0.06}F_{0.25}O_{0.84}Cl_{0.02}Li_{0.38} \rightarrow Ti_3C_2(OH)_{0.06}F_{0.116}O_{0.84}Cl_{0.02}Li_{0.246} + 0.134Li^+ + 0.134F^- \quad (8)$$

It is generally assumed that the ion exchange occurs between the solution and ions located between the MXene layers. If this assumption of simple ion exchange is correct, the number of intercalating ions in the MXene must be equal to that of the ions released to the solution. In 1 M NaCl, close to complete ion exchange was achieved and there is very little Li^+ remaining in the exchanged MXene, while, in 1 M KCl, many Li^+ ions coexist with K^+ ions. It is perhaps surprising that, although the exchange in KCl is exothermic and that in NaCl is endothermic, the extent of exchange in NaCl is much greater than in KCl. It clearly indicates that both kinetic and thermodynamic factors are playing a role. It is possible that the K^+ ions in the interlayers being more strongly bound are less mobile than the more weakly bound Na^+ ions. Thus, their overall diffusion and exchange rates might be slower.

In addition, in 1 M LiCl, there is assumed to be no net intercalation because of zero driving force for lithium replacing lithium. However, in nanopure water, Li^+ ions deintercalate and F^- ions most likely participate to charge balance the reaction. Protons are also exchanged with Li^+ and other ions and are responsible for a decrease in the pH of the solution (see Table S2 for the moles of H^+ ions released), but we neglected their contribution in the enthalpy of the above reactions because the number of protons released is very small. We conclude that, in addition to alkali cations, protons and anions such as F^- may also participate in the ion exchange process to charge balance the overall reaction.

On the basis of these reactions, the exchange enthalpies (per mole of exchanged ions) between MXene and an aqueous solution containing alkali ions are described in Tables S6 and S7 in the Supporting Information and are summarized in Table 2.

Table 2. Exchange Enthalpies (kJ/mol of Exchanged Ions) of HCl-LiF Etched MXene with Deionized Water and 1 M Alkali Chloride Solutions at 25 °C

	ΔH_{ex}[a] (kJ/mol)	
solution	measured composition	corrected composition
1 M KCl	−9.3 ± 2.2	−11.0 ± 2.4
1 M NaCl	21.0 ± 0.9	20.4 ± 0.9
1 M LiCl	−1.3 ± 0.2	−1.3 ± 0.2
nanopure H_2O	302.4 ± 0.6	301.9 ± 0.6

[a] ΔH_{ex} = Enthalpy of exchange.

The calculated exchange enthalpy for the measured and corrected MXene compositions is moderately exothermic for K−Li exchange but is endothermic for Na−Li exchange. The very slightly exothermic value in 1 M LiCl may reflect a small amount of proton exchange. The apparent exchange enthalpy is highly endothermic in nanopure water which is expected because Li^+ and F^- ions are both deintercalating from the MXene layers into the solution (see Tables S6 and S7 in the Supporting Information). The exchange enthalpies for K^+, Na^+, and Li^+ for the corrected MXene follow a similar trend as shown for the measured composition. The slight differences

DOI: 10.1021/acs.jpcc.7b02419
J. Phys. Chem. C 2017, 121, 15145−15153

reflect the difference in molecular weight of the MXene used in the calculation.

The driving force for deintercalation is presumably the larger entropy associated with ions free in solution compared to those confined in the interlayers. Conversely, intercalation probably involves a decrease of entropy, offsetting some of the energetic stabilization. Ion exchange, with the same number of ions at the beginning and end of the process, will have smaller entropy effects than a reaction, which intercalates or deintercalates a net number of ions. The energetic driving force for K^+-Li^+ exchange is exothermic, while that for Na^+-Li^+ exchange is endothermic. This may suggest more favorable electrostatic bonding interaction of the K^+ ions with the negatively charged species (OH^-/F^-) present in the interlayers. The hydration radius for K^+ is smaller than that for Na^+.[56] This appears consistent with the larger extent of K exchange and the more exothermic enthalpy of exchange. More specific geometric and structural factors, as yet not clearly known, may also play a role.

Many reports have addressed the effect of intercalation of different ions on electrochemical performance and change in the interplanar spacing of the MXene layers. The first report by Naguib et al.[16] on Li^+ intercalation showed an increase in the *c*-lattice parameter by almost 19.5%, indicating intercalation of Li between the MXene layers. Dall'Agnese et al. reported an increase of 4.6 Å in the *c*-lattice parameter with Na^+ intercalation into the V_2CT_x layers.[57] For both studies, organic electrolytes were used. Using electrochemical atomic force microscopy, Come et al.[58] showed a contraction associated with Li^+, Na^+, and Mg^{2+} intercalation upon electrochemical cycling in aqueous electrolytes. This appears to be different from conventional electrodes or even for MXenes in organic electrolytes where redox intercalation results in volumetric expansion. Fredrickson et al.[59] found there are different stable sites for H, OH, O, H_2, and H_2O. The *c*-lattice parameter varies significantly with the functionalization of the MXene and is greatly increased upon intercalation of water. Ghidiu et al.[29] studied the cation exchange of Li^+ with Na^+, K^+, Rb^+, Mg^{2+}, and Ca^{2+}. The results suggested that expansion of interplanalar spacing is caused by water associated with these cations. The above studies suggest that ion exchange is a complex process, and the differences between the hydration state of cations in the MXene and in the aqueous solution, rather than simply the hydration state in one phase, may influence the enthalpy of ion exchange. The findings from Osti et al.[30] suggest that intercalation of K^+ yields a MXene with more uniform, homogeneous structure that holds more stable water between the individual MXene layers, thereby increasing the stability of the MXene. Our findings are consistent with this observation.

CONCLUSIONS

Water vapor adsorption calorimetry suggests minimal interactions of water in a clay-like MXene. Immersion calorimetry of clay-like $Ti_3C_2T_x$ supports minimal interaction with pure water. Ion exchange upon immersion in alkali metal chloride solution has been confirmed. Potassium–lithium exchange is exothermic (ΔH_{ex} = −9.3 (±2.2) kJ/mol of MXene), while sodium lithium exchange is endothermic (ΔH_{ex} = 21.0 (±0.9) kJ/mol of MXene). Deintercalation of lithium (accompanied by fluoride) is strongly endothermic (ΔH_{ex} = 302.4 (±0.6) kJ/mol of MXene). We propose that one should consider the energetics of intercalated species, which will alter the MXene properties, as potentially important variables to control and tune ion transport and capacity in MXenes used in Li-ion batteries, supercapacitors, and other applications.

ASSOCIATED CONTENT

Supporting Information

The Supporting Information is available free of charge on the ACS Publications website at DOI: 10.1021/acs.jpcc.7b02419.

Figure showing XRD patterns of HF and HCl-LiF etched samples and tables showing the elemental composition of clay-like MXene, the pH of the solutions before and after the immersion experiment and moles of H^+ released from clay-MXene, ICP-MS data analysis, and exchange enthalpies (PDF)

AUTHOR INFORMATION

Corresponding Author

*E-mail: anavrotsky@ucdavis.edu. Phone: (530) 752-3292.

ORCID

Yury Gogotsi: 0000-0001-9423-4032

Alexandra Navrotsky: 0000-0002-3260-0364

Di Wu: 0000-0001-6879-321X

Notes

The authors declare no competing financial interest.

ACKNOWLEDGMENTS

This work was supported by the Fluid Interface Reactions, Structures and Transport, an Energy Frontier Research Center funded by the U.S. Department of Energy, Office of Science, Office of Basic Energy Sciences under Award Number 4000134953.

REFERENCES

(1) Stankovich, S.; Dikin, D. A.; Piner, R. D.; Kohlhaas, K. A.; Kleinhammes, A.; Jia, Y.; Wu, Y.; Nguyen, S. T.; Ruoff, R. S. Synthesis of Graphene-Based Nanosheets via Chemical Reduction of Exfoliated Graphite Oxide. *Carbon* **2007**, *45*, 1558–1565.

(2) Lin, Y.; Williams, T. V.; Connell, J. W. Soluble, Exfoliated Hexagonal Boron Nitride Nanosheets. *J. Phys. Chem. Lett.* **2010**, *1*, 277–283.

(3) Eda, G.; Yamaguchi, H.; Voiry, D.; Fujita, T.; Chen, M.; Chhowalla, M. Photoluminescence from Chemically Exfoliated MoS_2. *Nano Lett.* **2011**, *11*, 5111–5116.

(4) Naguib, M.; Mochalin, V. N.; Barsoum, M. W.; Gogotsi, Y. 25th Anniversary Article: MXenes: A New Family of Two-Dimensional Materials. *Adv. Mater.* **2014**, *26*, 992–1005.

(5) Naguib, M.; Gogotsi, Y. Synthesis of Two-Dimensional Materials by Selective Extraction. *Acc. Chem. Res.* **2015**, *48*, 128–135.

(6) Naguib, M.; Kurtoglu, M.; Presser, V.; Lu, J.; Niu, J.; Heon, M.; Hultman, L.; Gogotsi, Y.; Barsoum, M. W. Two-Dimensional Nanocrystals Produced by Exfoliation of Ti_3AlC_2. *Adv. Mater.* **2011**, *23*, 4248–4253.

(7) Anasori, B.; Lukatskaya, M. R.; Gogotsi, Y. 2D Metal Carbides and Nitrides (MXenes) for Energy Storage. *Nat. Rev. Mater.* **2017**, *2*, 16098.

(8) Mashtalir, O.; Naguib, M.; Mochalin, V. N.; Dall'Agnese, Y.; Heon, M.; Barsoum, M. W.; Gogotsi, Y. Intercalation and Delamination of Layered Carbides and Carbonitrides. *Nat. Commun.* **2013**, *4*, 1716.

(9) Naguib, M.; Unocic, R. R.; Armstrong, B. L.; Nanda, J. Large-Scale Delamination of Multi-Layers Transition Metal Carbides and Carbonitrides "MXenes. *Dalton Trans.* **2015**, *44*, 9353–9358.

(10) Halim, J.; Cook, K. M.; Naguib, M.; Eklund, P.; Gogotsi, Y.; Rosen, J.; Barsoum, M. W. X-ray Photoelectron Spectroscopy of Select

Multi-Layered Transition Metal Carbides (MXenes). *Appl. Surf. Sci.* **2016**, *362*, 406−417.
(11) Hope, M. A.; Forse, A. C.; Griffith, K. J.; Lukatskaya, M. R.; Ghidiu, M.; Gogotsi, Y.; Grey, C. P. NMR Reveals the Surface Functionalisation of Ti_3C_2 MXene. *Phys. Chem. Chem. Phys.* **2016**, *18*, 5099−5102.
(12) Wang, H. W.; Naguib, M.; Page, K.; Wesolowski, D. J.; Gogotsi, Y. Resolving the Structure of $Ti_3C_2T_x$ MXenes through Multilevel Structural Modeling of the Atomic Pair Distribution Function. *Chem. Mater.* **2016**, *28*, 349−359.
(13) Yoo, E.; Kim, J.; Hosono, E.; Zhou, H. S.; Kudo, T.; Honma, I. Large Reversible Li Storage of Graphene Nanosheet Families for Use in Rechargeable Lithium Ion Batteries. *Nano Lett.* **2008**, *8*, 2277−2282.
(14) Xiao, J.; Choi, D.; Cosimbescu, L.; Koech, P.; Liu, J.; Lemmon, J. P. Exfoliated MoS_2 Nanocomposite as an Anode Material for Lithium Ion Batteries. *Chem. Mater.* **2010**, *22*, 4522−4524.
(15) Naguib, M.; Mashtalir, O.; Carle, J.; Presser, V.; Lu, J.; Hultman, L.; Gogotsi, Y.; Barsoum, M. W. Two-Dimensional Transition Metal Carbides. *ACS Nano* **2012**, *6*, 1322−1331.
(16) Naguib, M.; Come, J.; Dyatkin, B.; Presser, V.; Taberna, P. L.; Simon, P.; Barsoum, M. W.; Gogotsi, Y. MXene: A Promising Transition Metal Carbide Anode for Lithium-Ion Batteries. *Electrochem. Commun.* **2012**, *16*, 61−64.
(17) Ghidiu, M.; Lukatskaya, M. R.; Zhao, M. Q.; Gogotsi, Y.; Barsoum, M. W. Conductive Two-Dimensional Titanium Carbide 'Clay' with High Volumetric Capacitance. *Nature* **2014**, *516*, 78−81.
(18) Lukatskaya, M. R.; Mashtalir, O.; Ren, C. E.; Dall'Agnese, Y.; Rozier, P.; Taberna, P. L.; Naguib, M.; Simon, P.; Barsoum, M. W.; Gogotsi, Y. Cation Intercalation and High Volumetric Capacitance of Two-Dimensional Titanium Carbide. *Science* **2013**, *341*, 1502−1505.
(19) Halim, J.; Kota, S.; Lukatskaya, M. R.; Naguib, M.; Zhao, M. Q.; Moon, E. J.; Pitock, J.; Nanda, J.; May, S. J.; Gogotsi, Y. Synthesis and Characterization of 2D Molybdenum Carbide (MXene). *Adv. Funct. Mater.* **2016**, *26*, 3118−3127.
(20) Mashtalir, O.; Lukatskaya, M. R.; Zhao, M. Q.; Barsoum, M. W.; Gogotsi, Y. Amine-Assisted Delamination of Nb_2C MXene for Li-Ion Energy Storage Devices. *Adv. Mater.* **2015**, *27*, 3501−3506.
(21) Luo, J.; Tao, X.; Zhang, J.; Xia, Y.; Huang, H.; Zhang, L.; Gan, Y.; Liang, C.; Zhang, W. Sn^{4+} Ion Decorated Highly Conductive Ti_3C_2 MXene: Promising Lithium-Ion Anodes with Enhanced Volumetric Capacity and Cyclic Performance. *ACS Nano* **2016**, *10*, 2491−2499.
(22) Ren, C. E.; Zhao, M.; Makaryan, T.; Halim, J.; Boota, M.; Kota, S.; Anasori, B.; Barsoum, M. W.; Gogotsi, Y. Porous Two-Dimensional Transition Metal Carbide (MXene) Flakes for High-Performance Li-Ion Storage. *ChemElectroChem* **2016**, *3*, 689−693.
(23) Zhao, M. Q.; Torelli, M.; Ren, C. E.; Ghidiu, M.; Ling, Z.; Anasori, B.; Barsoum, M. W.; Gogotsi, Y. 2D Titanium Carbide and Transition Metal Oxides Hybrid Electrodes for Li-Ion Storage. *Nano Energy* **2016**, *30*, 603−613.
(24) Xie, Y.; Naguib, M.; Mochalin, V. N.; Barsoum, M. W.; Gogotsi, Y.; Yu, X.; Nam, K. W.; Yang, X. Q.; Kolesnikov, A. I.; Kent, P. R. C. Role of Surface Structure on Li-Ion Energy Storage Capacity of Two-Dimensional Transition-Metal Carbides. *J. Am. Chem. Soc.* **2014**, *136*, 6385−6394.
(25) Sun, D.; Hu, Q.; Chen, J.; Zhang, X.; Wang, L.; Wu, Q.; Zhou, A. Structural Transformation of MXene (V_2C, Cr_2C, and Ta_2C) with O Groups during Lithiation: A First-Principles Investigation. *ACS Appl. Mater. Interfaces* **2016**, *8*, 74−81.
(26) Yang, E.; Ji, H.; Kim, J.; Kim, H.; Jung, Y. Exploring the Possibilities of Two-Dimensional Transition Metal Carbides as Anode Materials for Sodium Batteries. *Phys. Chem. Chem. Phys.* **2015**, *17*, 5000−5005.
(27) Tang, Q.; Zhou, Z.; Shen, P. Are MXenes Promising Anode Materials for Li Ion Batteries? Computational Studies on Electronic Properties and Li Storage Capability of Ti_3C_2 and $Ti_3C_2X_2$ (X= F, OH) Monolayer. *J. Am. Chem. Soc.* **2012**, *134*, 16909−16916.
(28) Xie, Y.; Naguib, M.; Mochalin, V. N.; Barsoum, M. W.; Gogotsi, Y.; Yu, X.; Nam, K. W.; Yang, X. Q.; Kolesnikov, A. I.; Kent, P. R. Role of Surface Structure on Li-Ion Energy Storage Capacity of Two-Dimensional Transition-Metal Carbides. *J. Am. Chem. Soc.* **2014**, *136*, 6385−6394.
(29) Ghidiu, M.; Halim, J.; Kota, S.; Bish, D.; Gogotsi, Y.; Barsoum, M. W. Ion-Exchange and Cation Solvation Reactions in Ti_3C_2 MXene. *Chem. Mater.* **2016**, *28*, 3507−3514.
(30) Osti, N. C.; Naguib, M.; Ostadhossein, A.; Xie, Y.; Kent, P. R.; Dyatkin, B.; Rother, G.; Heller, W. T.; van Duin, A. C.; Gogotsi, Y. Effect of Metal Ion Intercalation on the Structure of MXene and Water Dynamics on its Internal Surfaces. *ACS Appl. Mater. Interfaces* **2016**, *8*, 8859−8863.
(31) Kajiyama, S.; Szabova, L.; Sodeyama, K.; Iinuma, H.; Morita, R.; Gotoh, K.; Tateyama, Y.; Okubo, M.; Yamada, A. Sodium-Ion Intercalation Mechanism in MXene Nanosheets. *ACS Nano* **2016**, *10*, 3334−3341.
(32) Mashtalir, O.; Lukatskaya, M.; Kolesnikov, A.; Raymundo-Piñero, E.; Naguib, M.; Barsoum, M.; Gogotsi, Y. The Effect of Hydrazine Intercalation on the Structure and Capacitance of 2D Titanium Carbide (MXene). *Nanoscale* **2016**, *8*, 9128−9133.
(33) Ahmed, B.; Anjum, D. H.; Hedhili, M. N.; Gogotsi, Y.; Alshareef, H. N. H_2O_2 Assisted Room Temperature Oxidation of Ti_2C MXene for Li-Ion Battery Anodes. *Nanoscale* **2016**, *8*, 7580−7587.
(34) Yu, Y. X. Prediction of Mobility, Enhanced Storage Capacity, and Volume Change during Sodiation on Interlayer-Expanded Functionalized Ti_3C_2 MXene Anode Materials for Sodium-Ion Batteries. *J. Phys. Chem. C* **2016**, *120*, 5288−5296.
(35) Ren, C. E.; Hatzell, K. B.; Alhabeb, M.; Ling, Z.; Mahmoud, K. A.; Gogotsi, Y. Charge-and Size-Selective Ion Sieving Through $Ti_3C_2T_x$ MXene Membranes. *J. Phys. Chem. Lett.* **2015**, *6*, 4026−4031.
(36) Sun, H.; Wu, D.; Guo, X.; Shen, B.; Liu, J.; Navrotsky, A. Energetics of Confinement of n-Hexane in Ca−Na Ion Exchanged Zeolite A. *J. Phys. Chem. C* **2014**, *118*, 25590−25596.
(37) Vernimmen, J.; Guidotti, M.; Silvestre-Albero, J.; Jardim, E. O.; Mertens, M.; Lebedev, O. I.; Van Tendeloo, G.; Psaro, R.; Rodríguez-Reinoso, F.; Meynen, V.; Cool, P. Immersion Calorimetry as a Tool To Evaluate the Catalytic Performance of Titanosilicate Materials in the Epoxidation of Cyclohexene. *Langmuir* **2011**, *27*, 3618−3625.
(38) Wu, D.; McDonald, T. M.; Quan, Z.; Ushakov, S. V.; Zhang, P.; Long, J. R.; Navrotsky, A. Thermodynamic Complexity of Carbon Capture in Alkylamine-Functionalized Metal-Organic Frameworks. *J. Mater. Chem. A* **2015**, *3*, 4248−4254.
(39) Radha, S.; Navrotsky, A. Energetics of CO_2 Adsorption on Mg−Al Layered Double Hydroxides and Related Mixed Metal Oxides. *J. Phys. Chem. C* **2014**, *118*, 29836−29844.
(40) Wu, D.; Guo, X.; Sun, H.; Navrotsky, A. Energy Landscape of Water and Ethanol on Silica Surfaces. *J. Phys. Chem. C* **2015**, *119*, 15428−15433.
(41) Wu, D.; Navrotsky, A. Thermodynamics of Metal-Organic Frameworks. *J. Solid State Chem.* **2015**, *223*, 53−58.
(42) Shivaramaiah, R.; Navrotsky, A. Energetics of Order−Disorder in Layered Magnesium Aluminum Double Hydroxides with Interlayer Carbonate. *Inorg. Chem.* **2015**, *54*, 3253−3259.
(43) Wu, D.; Navrotsky, A. Small Molecule−Silica Interactions in Porous Silica Structures. *Geochim. Cosmochim. Acta* **2013**, *109*, 38−50.
(44) Sharma, G.; Naguib, M.; Feng, D.; Gogotsi, Y.; Navrotsky, A. Calorimetric Determination of Thermodynamic Stability of MAX and MXene Phases. *J. Phys. Chem. C* **2016**, *120*, 28131−28137.
(45) Ushakov, S. V.; Navrotsky, A. Direct Measurements of Water Adsorption Enthalpy on Hafnia and Zirconia. *Appl. Phys. Lett.* **2005**, *87*, 164103.
(46) Liu, F.; Zhou, A.; Chen, J.; Zhang, H.; Cao, J.; Wang, L.; Hu, Q. Preparation and Methane Adsorption of Two-Dimensional Carbide Ti_2C. *Adsorption* **2016**, *22*, 915−922.
(47) Liang, X.; Garsuch, A.; Nazar, L. F. Sulfur Cathodes Based on Conductive MXene Nanosheets for High-Performance Lithium−Sulfur Batteries. *Angew. Chem., Int. Ed.* **2015**, *54*, 3907−3911.
(48) Fard, A. K.; Mckay, G.; Chamoun, R.; Rhadfi, T.; Preud'Homme, H.; Atieh, M. A. Barium Removal from Synthetic

DOI: 10.1021/acs.jpcc.7b02419
J. Phys. Chem. C 2017, 121, 15145−15153

Natural and Produced Water using MXene as Two Dimensional (2-D) Nanosheet Adsorbent. *Chem. Eng. J.* **2017**, *317*, 331−342.
(49) Ling, Z.; Ren, C. E.; Zhao, M. Q.; Yang, J.; Giammarco, J. M.; Qiu, J.; Barsoum, M. W.; Gogotsi, Y. Flexible and Conductive MXene Films and Nanocomposites with High Capacitance. *Proc. Natl. Acad. Sci. U. S. A.* **2014**, *111*, 16676−16681.
(50) Xiao, B.; Li, Y.; Yu, X.; Cheng, J. MXenes: Reusable Materials for NH_3 Sensor or Capturer by Controlling the Charge Injection. *Sens. Actuators, B* **2016**, *235*, 103−109.
(51) Yu, X.; Li, Y.; Cheng, J.; Liu, Z.; Li, Q.; Li, W.; Yang, X.; Xiao, B. Monolayer Ti_2CO_2: A Promising Candidate for NH_3 Sensor or Capturer with High Sensitivity and Selectivity. *ACS Appl. Mater. Interfaces* **2015**, *7*, 13707−13713.
(52) Gao, G.; O'Mullane, A. P.; Du, A. 2D MXenes: A New Family of Promising Catalysts for the Hydrogen Evolution Reaction. *ACS Catal.* **2017**, *7*, 494−500.
(53) Liu, Y.; Du, H.; Zhang, X.; Yang, Y.; Gao, M.; Pan, H. Superior Catalytic Activity Derived from a Two-Dimensional Ti_3C_2 Precursor Towards the Hydrogen Storage Reaction of Magnesium Hydride. *Chem. Commun.* **2016**, *52*, 705−708.
(54) Azofra, L. M.; Li, N.; MacFarlane, D. R.; Sun, C. Promising Prospects for 2D d^2−d^4 M_3C_2 Transition Metal Carbides (MXenes) in N_2 Capture and Conversion into Ammonia. *Energy Environ. Sci.* **2016**, *9*, 2545−2549.
(55) Shannon, R. D. Revised Effective Ionic Radii and Systematic Studies of Interatomic Distances in Halides and Chalcogenides. *Acta Crystallogr., Sect. A: Cryst. Phys., Diffr., Theor. Gen. Crystallogr.* **1976**, *32*, 751−767.
(56) Yang, Z. H. The Size and Structure of Selected Hydrated Ions and Implications for Ion Channel Selectivity. *RSC Adv.* **2015**, *5*, 1213−1219.
(57) Dall'Agnese, Y.; Taberna, P. L.; Gogotsi, Y.; Simon, P. Two-Dimensional Vanadium Carbide (MXene) as Positive Electrode for Sodium-Ion Capacitors. *J. Phys. Chem. Lett.* **2015**, *6*, 2305−2309.
(58) Come, J.; Black, J. M.; Lukatskaya, M. R.; Naguib, M.; Beidaghi, M.; Rondinone, A. J.; Kalinin, S. V.; Wesolowski, D. J.; Gogotsi, Y.; Balke, N. Controlling The Actuation Properties of MXene Paper Electrodes upon Cation Intercalation. *Nano Energy* **2015**, *17*, 27−35.
(59) Fredrickson, K. D.; Anasori, B.; Seh, Z. W.; Gogotsi, Y.; Vojvodic, A. Effects of Applied Potential and Water Intercalation on the Surface Chemistry of Ti_2C and Mo_2C MXenes. *J. Phys. Chem. C* **2016**, *120*, 28432−28440.

DOI: 10.1021/acs.jpcc.7b02419
J. Phys. Chem. C 2017, 121, 15145−15153